

CHAPTER 156

Nearshore Current Patterns on Barred Beaches

David G. Hazen*, Brian Greenwood†, and Anthony J. Bowen*

INTRODUCTION

The last few years have been marked by a renewed interest in the old concept of undertow, the seaward flow which balances the surface flux of water associated with waves, particularly with breaking waves (Svendsen, 1984; Stive and Wind, 1986; etc.). This is clearly an important current in terms of the sedimentary processes which determine the beach profile. Roelvink and Stive have provided laboratory data that suggests the profile results from a net balance between three main factors; the wave skewness, the undertow, and the beach slope. However, in the field the third dimension, the longshore direction, may play a significant role. Even if the system is assumed uniform alongshore, strong longshore currents certainly influence the mobility of the sediment and may play more complex roles, in generating shear waves for example.

It seems appropriate to represent the system, both on/offshore and alongshore, in one self-consistent model. Recent work has been clearly progressing in this direction (Stive and DeVriend, 1987; Svendsen and Lorenz, 1989). It is therefore also appropriate at this stage to look at existing field data to see how well one can define trends that the modelling results should reproduce.

There are some very clear limitations. In the field it is difficult to describe, in any detail, the longshore variability. Small hydraulic gradients in the alongshore direction may drive longshore currents, rip currents, or some general nearshore circulation associated with larger scale topography. Even in a relatively 2-D situation, it is known that the longshore currents are strongly dependent on the directional distribution of the wave spectrum, a factor which is hard to estimate well, unless the angle of wave approach is large.

The measurements here were taken on a beach at the end of a large bay of restricted width. Large waves can only be generated along the long axis of

* Department of Oceanography, Dalhousie University, Halifax, Nova Scotia B3H 4J1, Canada

† Department of Geography, Scarborough College, University of Toronto, Scarborough, Ontario M1C 1A4, Canada

the system, so that the angles of wave approach relative to the beach tend to be small ($0 - 15^\circ$). Attention is therefore focussed primarily on the on-offshore structure of the flow.

FIELD MEASUREMENTS

The Canadian Coastal Sediment Transport (C-COAST) experiments have taken place over the past three years. These experiments involved the deployment of arrays of up to twenty electromagnetic current meters, ten pressure sensors and an assortment of wave-wires and suspended sediment sensors from the shoreline seawards to a depth of $5 - 7m$. Each of the experiments acquired data during periods of higher wave activity over a period of approximately one month under varying wave conditions. The sites included a two dimensional beach (Queensland, Nova Scotia in 1988), a barred beach with normally incident waves (Bluewater, Ontario in 1987 and 1988) and a multibarred beach with

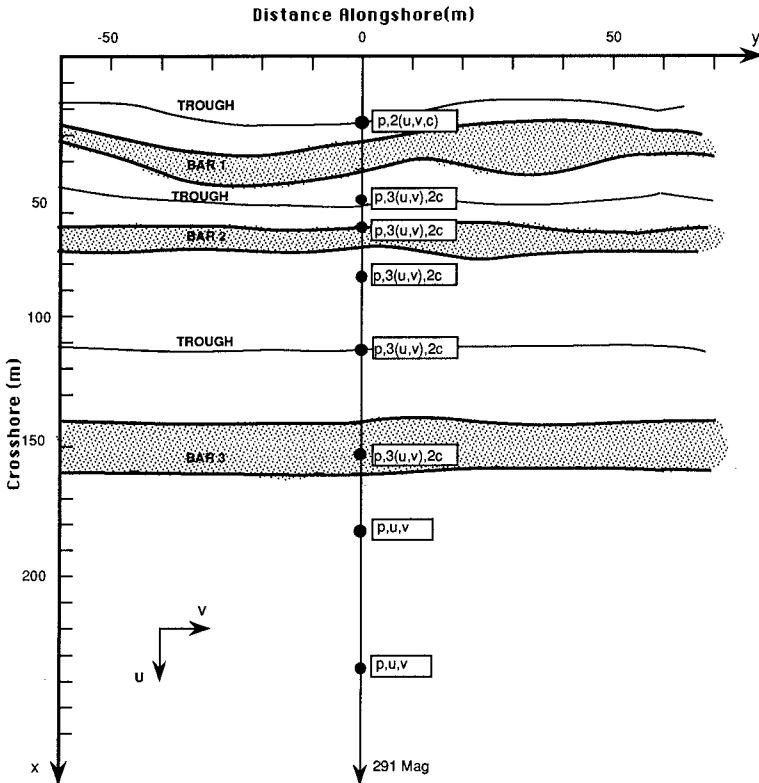


Figure 1. Bluewater 1988 Instrument Schematic showing locations of pressure sensors (p), two component flowmeters (u, v) and optical backscatter suspended sediment concentration sensors (c).

normal or obliquely incident waves (Stanhope Lane, PEI in 1989). The data discussed in this paper will be primarily from the 1988 Bluewater experiment, which took place in May and June of that year.

The data are gathered from a cross-shore array of pressure gauges ('p'), two component flowmeters ('u' and 'v') and optical backscatter suspended sediment concentration sensors ('c'). These instruments were located as shown in Figure 1 with co-ordinate systems as indicated. The sensors were orientated and connected to the hard-wired UDATS data acquisition system (Hazen *et al.*, 1987). Additional sensors were deployed to record wind speed and direction, concentration profiles by acoustic backscatter, depth of sedimentary activity and to collect physical samples of suspended sediment for concentration and grain size measurement.

Detailed analysis of the current data is limited by the number of working flowmeters and the long periods of calm or offshore winds during the study. For these reasons, discussion will concentrate on data collected from flowmeters at 150m on the crest of bar 3 and flowmeters at 55m, just inshore of bar 2 (both at heights of 10 and 25cm above the bed) together with winds from a 10m tower erected adjacent to the beach.

The data base selected for the paper includes the most severe conditions encountered during the experiment (on June 9, 1988) and a period of wave conditions which were more typical of the wave conditions on the lake (June 16). In both cases the incident waves propagate slightly in the y -positive direction, the angle of incidence being $5-10^\circ$ on 9 June, $3-7^\circ$ on the 16th June. In both cases, the longshore current flows in the direction expected.

The conditions on June the 9th are shown in Figure 2 with the wind rising quickly at noon, reaching a steady velocity of about 12 kts. Visual observations included an estimated significant wave height of 0.8m and white capping to the horizon. Observations report short crested waves during the period of active generation. As the wind drops, the waves become longer crested but tend to disappear due to the size of the bay. The mean water level at the shore responds directly to the wind force changing by 20cm in a few hours. The incident wave frequency drops during the maximum of the wind event and then quickly reverts to its previous level. The mean currents track the wind and significant wave heights peaking at 0.3m/s longshore and 0.2m/s cross shore, based on 10 minute averages taken every 30 minutes. The vertical dashed line indicates the start of the data run used in Figures 5 and 7.

Conditions on June 16, however, are more typical of the lower energy events during the study. As shown in Figure 3, the winds averaged around 9 kts. The system responds quite quickly once a threshold wind velocity of 6-7 kts is exceeded with dips in the incident wave frequency, and a rise in the mean water level and mean currents. Again, the vertical dashed line refers to the start of the data run used in Figure 6.

Figure 4 shows the conditions across the surf zone at the peak of the event of 9 June, indicated by the dashed line on Fig. 2. The continuous lines in Figures

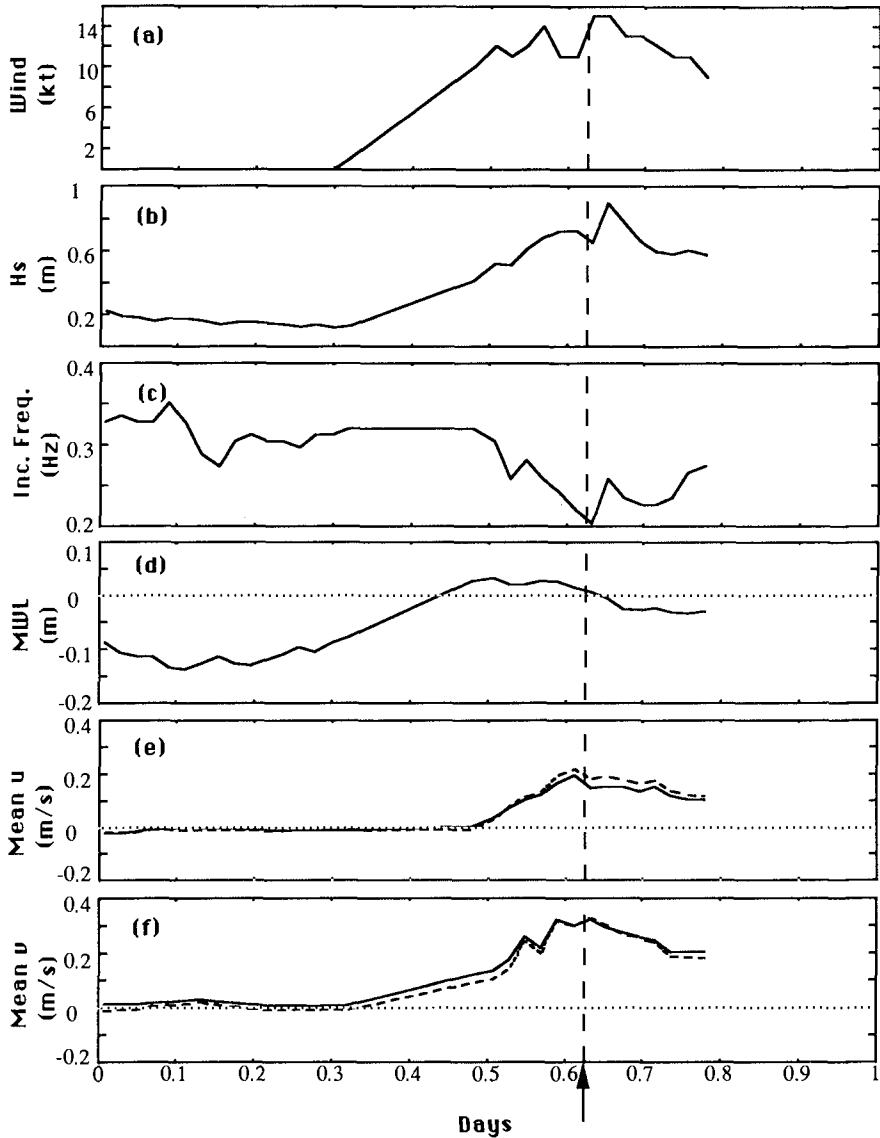


Figure 2. Conditions at Site on June 9, 1988. (a) wind speed, (b) significant wave height, (c) incident wave frequency, (d) mean water level, referenced to an arbitrary datum, (e) mean cross shore flow at 55m station. (Solid line is at 25cm above the bed while dashed line is at 10cm above the bed), (f) mean long shore flow at 55m (solid and dashed lines as in (e)). Vertical dashed line shows the beginning of the time used in Figures 4 and 7.

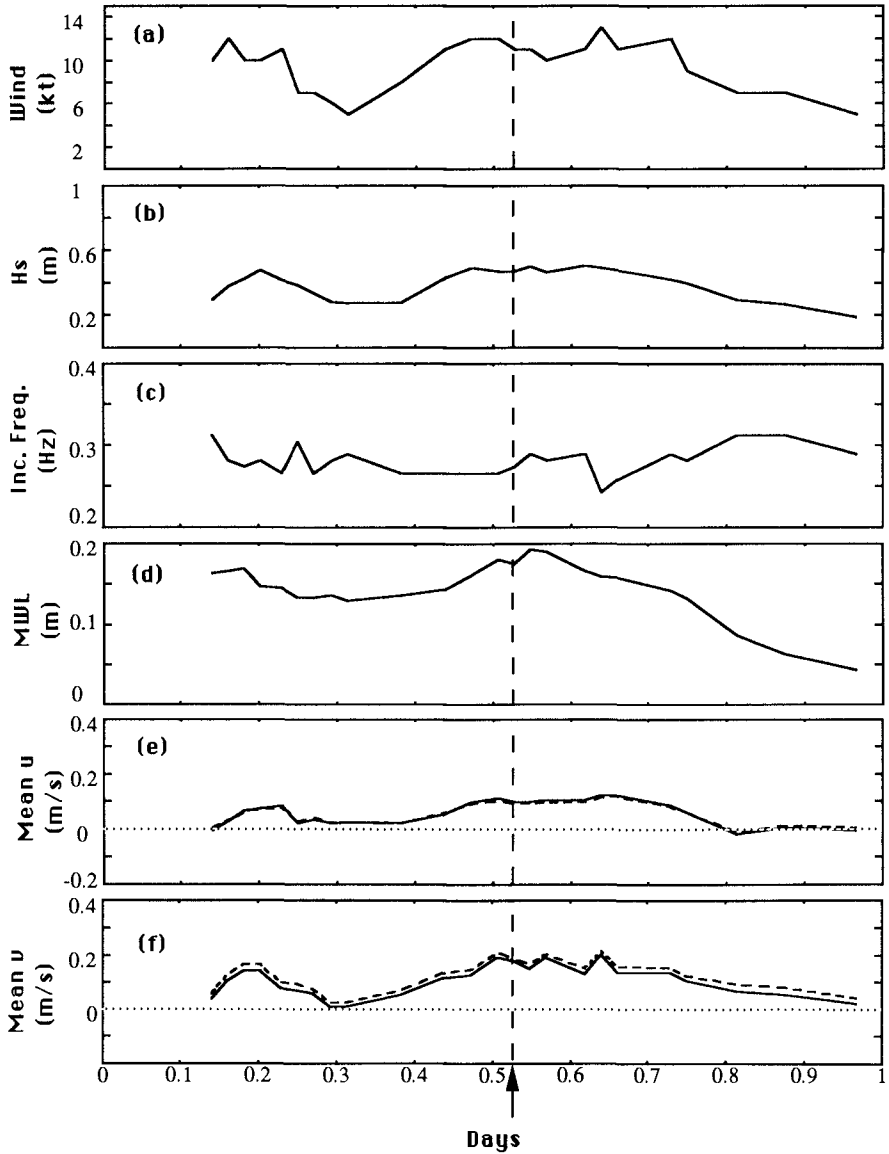


Figure 3. Conditions at Site on June 16, 1988. (a) wind speed, (b) significant wave height, (c) incident wave frequency, (d) mean water level, (e) mean cross-shore flow at 55m, (f) mean long shore flow at 55m. Vertical dashed line shows the beginning of the time period used in Figure 5.

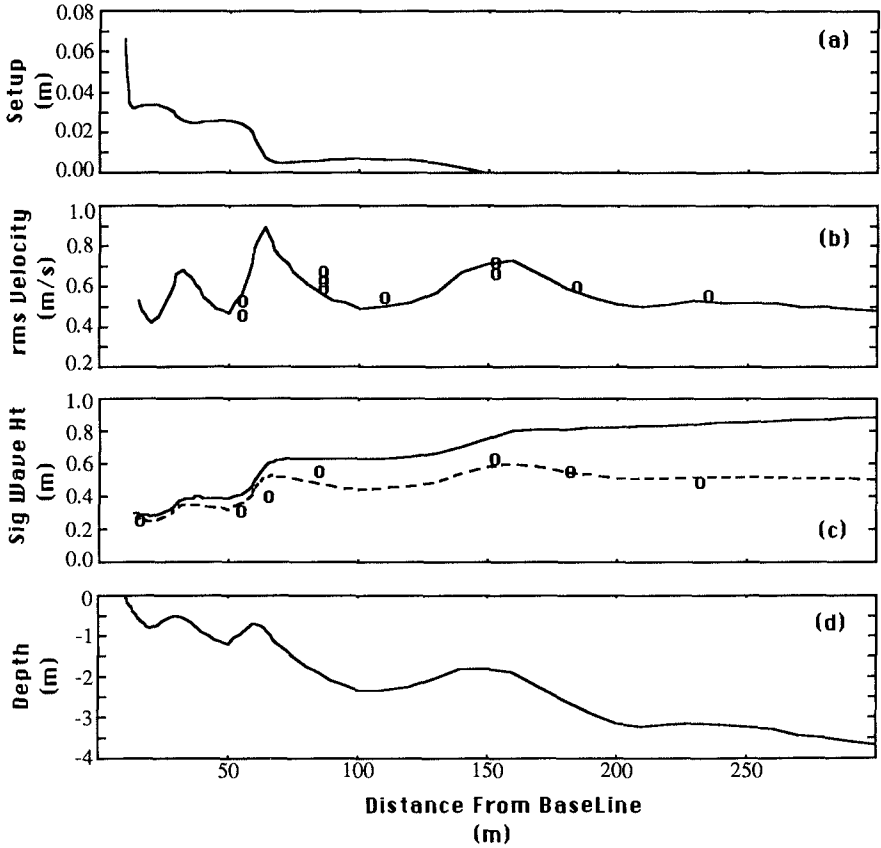


Figure 4. Cross Shore Profiles during June 9, 1988 'P4' data run, beginning at 1540. (a) predicted setup, (b) predicted and measured r.m.s. cross shore velocity, (c) predicted and measured significant wave height (dashed line indicates wave heights "uncorrected" to predict pressure gauge response, (d) measured depths.

4b and 4c show the theoretical distributions of on/offshore velocity, wave height and bottom pressure in the incident wave band, derived from a shoaling model based on Thornton and Guza (1983). The empirical parameters, used in such models are γ a ratio of wave height to water depth, and B a general dissipation constant. The results in Figure 4 are for $\gamma = 0.45$, $B = 1$ typical of values used in modelling wave evolution on open ocean beaches. The superimposed data points are from the flowmeter array (Fig. 4b) and the near-bed pressure gauges (Fig. 4c). The pressure has been expressed in terms of meters of water. Note that the pressure is not hydrostatic, the high wave frequencies found in the lake environment mean that the waves are in intermediate, not shallow, water until

very close to the shore.

The model, and the visual observations made during the field program, show that at the height of the storm there is some breaking on the third bar. Dissipation is generally low in the troughs and high on the inshore bars. Comparison with other model runs shows that the incident waves become saturated in the seaward face of the second bar if the incident waves are larger than about $0.4m$. As can be seen clearly in Figure 4b, the shoaling model predicts significant amplification of the wave orbital velocity over the bars, due to the depth dependent term in the linear theory. Whether this happens in reality is questionable, the model assumes that the rate of change of depth is slow, not a very good assumption even here where the incident frequency is high and the incident waves very short. However, the predicted amplification over bar three is clearly seen in the data. Inshore, the instrumental spacing does not allow a critical test of the model. The crests of the inshore bars were not used as instrument positions due to the very limited water depth above them.

Wave set-up was calculated in the dispersion model, the results shown in Fig. 4a. The predicted set-up is very small, a few centimeters. The general lake set-up (Fig. 2), of the order of $0.2m$ was much more noticeable. Measurements of set-up specifically were obtained by taking the difference between measurements for the inshore pressure gauges (and wave staffs) and the pressure gauge at $230m$. The results were somewhat scattered, the lake level changes being clearly seen at all stations, but the differences did not resolve the wave set-up with any accuracy, they confirmed that the set-up was small.

The model and data comparison for 1240 on the 16th of June, show a very similar picture (Fig. 5). The smaller wave height leads to less energy loss on the third bar, but breaking on the second bar results in a saturation condition and wave conditions inshore are essentially the same.

DISCUSSION

As shown in Figs. 2 and 3, the mean flows, averaged over 29 minutes, increase with increasing wave energy. In Figure 6, the seaward mean flow over the second bar ($55m$) and third bar ($150m$) are shown as a function of the incident wave height. For a significant wave height less than $0.25m$ the waves break only at the shoreline and the mean flows are very weak; if there is any tendency, it appears to be for onshore flow. As wave height increases, the mean flow at both positions increases more or less linearly with increasing waveheight.

Figure 6a shows the theoretical values for the set-up as a function of incident wave height and frequency. The field measurements scatter generally around these lines. The Thornton and Guza dissipation model includes a frequency dependence which results in a functional relationship for set-up which is weakly dependent on f . The set-up value shown is the predicted difference between the level at the third bar and that over the nearshore trough (cf. Figs. 4 and 5). The values reach a maximum, shown by the circles, when the surf zone becomes saturated, inshore from the third bar. Again, this wave height at

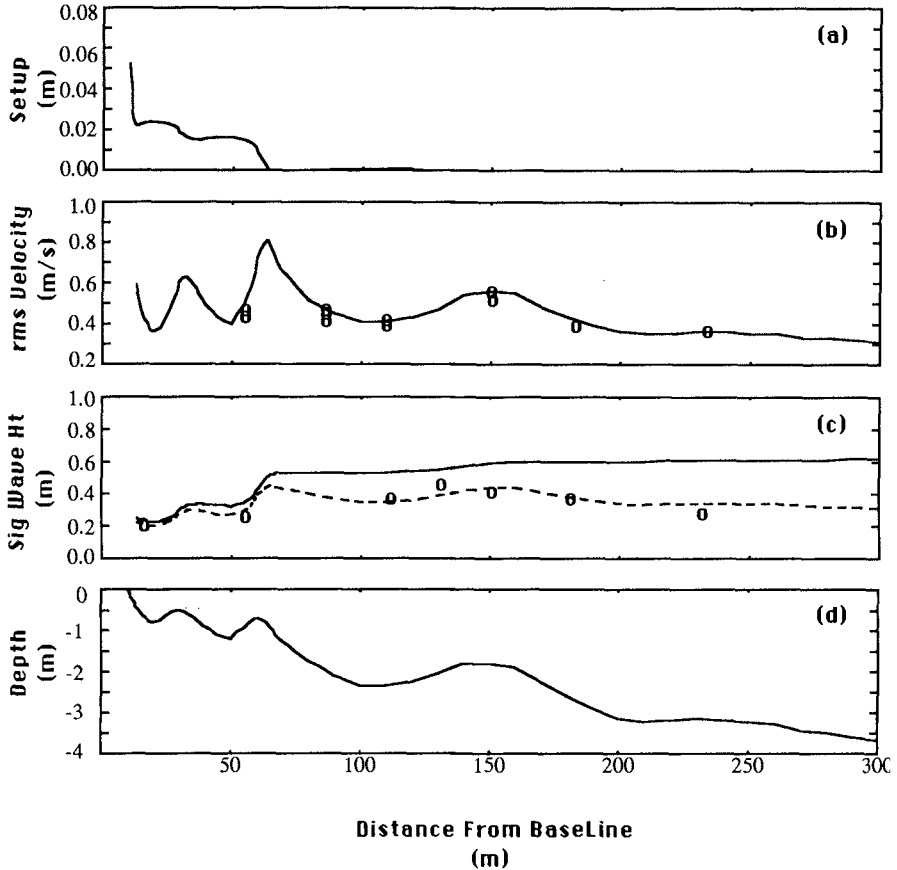


Figure 5. Cross Shore Profiles during June 16, 1988 'M4' data run, beginning at 1240. (a) predicted setup, (b) predicted and measured r.m.s. cross-shore velocity, (c) predicted and measured significant wave height (dashed line is wave height "uncorrected" to predict pressure gauge response), (d) measured depths.

which this occurs is weakly frequency dependent, but is of the order of 1.0m. Any further increase in wave height should merely raise the water level over the whole system, keeping the difference between these specific points constant.

In this particular situation, the set-up is so small that any further increase in set-up does not seriously change the hydrodynamic conditions inshore. The general change in water level due to the large scale wind effects is much more significant. The overall result is that the set-up reaches a definite maximum as should the undertow. Unfortunately, the wave conditions during the six week experiment did not exceed those shown in Fig. 2.

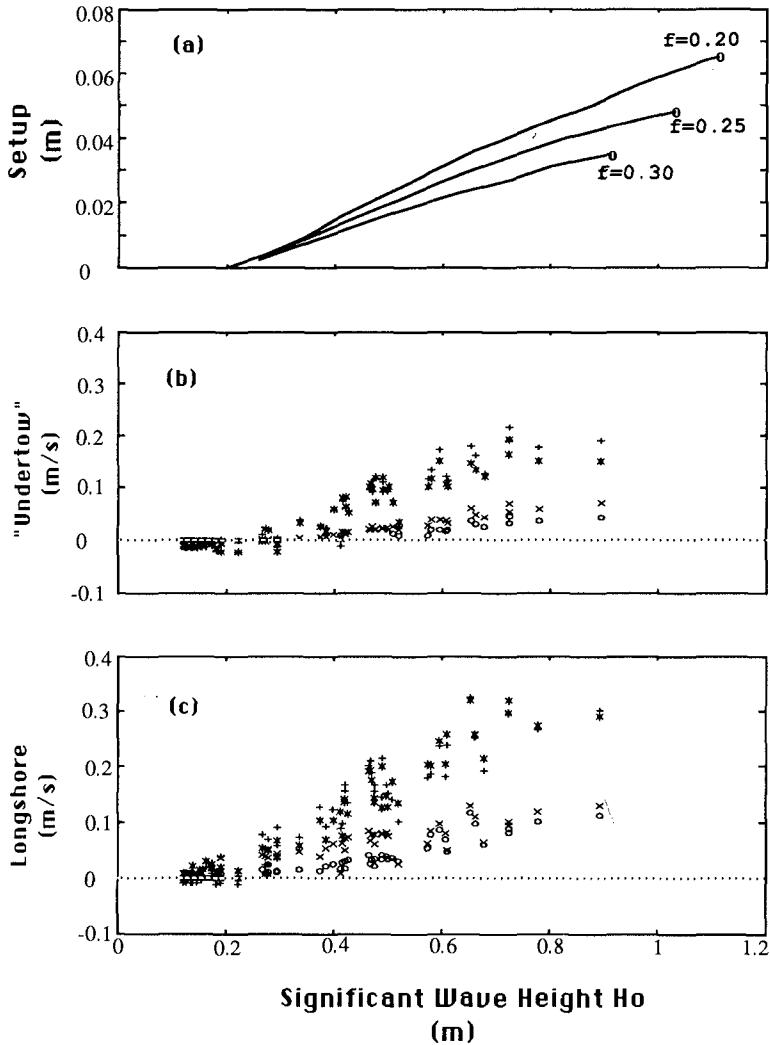


Figure 6. System Response to Various Incident Wave Heights (a) predicted setup at various frequencies (setup defined as (MWL @ 15m) - (MWL @ 150m)) (b) measured mean cross shore flow on June 9 and June 16 (+ = 55m, 10cm; * = 55m, 25cm; 0 = 150m, 10cm; x = 150m, 25cm), (c) measured mean longshore flow (symbols as in (b)).

The results do however show that the undertow continues to increase even though the wave conditions are *locally* saturated at the point of measurement. This occurs for $H_S \sim 0.5$ m at the 55m station. This is in contrast to the simple

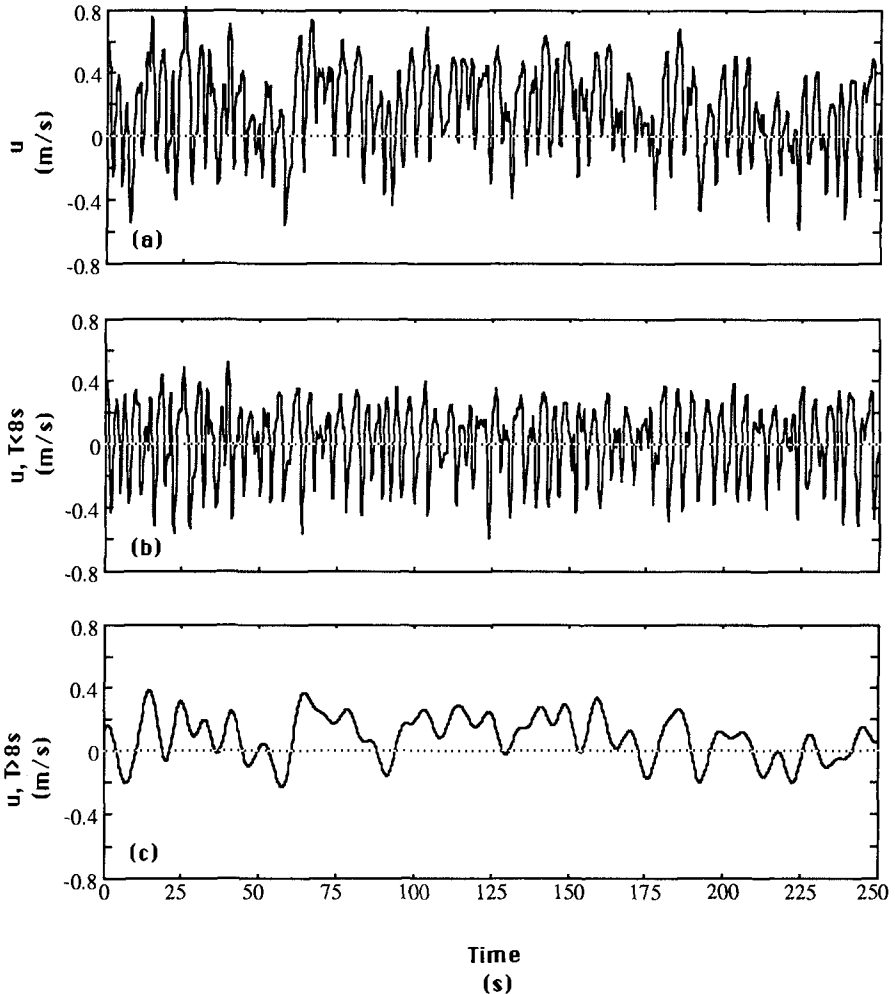


Figure 7. Time Series of Cross Shore Flow at 55m, 10cm height on June 9, 1988 beginning at 1540. (a) Time Series (b) Time series, high-pass filtered at 8 s (0.125 Hz) (c) Time Series, low pass filtered at 8 s (0.125 Hz).

models for plane beaches where the undertow depends primarily on the local conditions.

The discussion has thus far concentrated on the averages taken over a mean length of 29 minutes. This is a compromise between the need to take a reasonable number of points and the need to recognise that conditions at this beach change significantly on timescales of a few hours. However in using values for an analysis of beach equilibrium as in Roelvink and Stive (1989), care has to

be taken to include the motion at all time scales. The time variability seen at the on/offshore flow at the lower flowmeter at 55m is shown in Figure 7a. When this is filtered to separate out the incident waves, using a cut-off frequency of 0.125 Hz, the residual flow is seen (Fig. 7c) as being quite variable on a variety of time scales. While the mean is of over 0.2m/s, pulses in the residual reach 0.4m/s.

CONCLUSIONS

In this rather complex environment, a relatively simple dissipation model based on Thornton and Guza (1983) works reasonably well. Parameter values $\gamma = 0.45$, $B = 1$ suggest that the lake environment is behaving as an ocean environment, although the waves are short and steep there is a full (and rather broad) wave spectrum, tending to be rather short crested during periods of active generation when there are whitecaps to the horizon.

Measurements of the mean flow show a tendency for the flows to be very small during periods of low wave height, increasing approximately linearly with wave height once the waves begin to break on the outer bar. Saturation is predicted, if the motion is primary two-dimensional, for wave conditions slightly more severe than those observed.

The measurements of offshore flow, the undertow, show noticeable variability at all time scales. A factor to be taken into account in any modelling exercise where sediment transport is assumed to be some function of current raised to some power. In general, the wave dissipation over the bars offshore tends to reduce wave activity inshore so that the undertow, the longshore current, and the low frequency oscillations are of the same order of magnitude as the wave orbital velocities.

ACKNOWLEDGEMENTS

The primary funding for the C-COAST experiments came from NSERC (C) Strategic Grants to Greenwood and Bowen and A.E. Hay and Bowen. Additional infrastructure support was obtained from Petro-Canada Ltd. and various branches of the Government of Canada, including the Atmospheric Environment Service, the Atlantic Geoscience Centre, the Marine Environment Data Service, Parks Canada, and the Canadian Coast Guard.

REFERENCES

- Greenwood, B., P.D. Osborne, A.J. Bowen, D.G. Hazen and A.E. Hay. Nearshore sediment flux and bottom boundary dynamics: the Canadian Coastal Sediment Transport Programme (C-COAST). Proc. Twenty-Second Coastal Engineering Conference, ASCE, New York.
- Hazen, D.G., D.A. Huntley and A.J. Bowen, 1987. UDATS: A System for Measuring Nearshore Processes. *Proc. Oceans '87*, IEEE, New York, 993-997.

- Roelvink, J.A. and M.J.F. Stive, 1989. Bar-generating cross-shore flow mechanisms on a beach. *J. Geophys. Res.*, *94*, 4785-4800.
- Stive, M.J.F. and H.G. Wind, 1986. Cross-shore mean flow in the surf zone. *Coastal Engineering*, *10*, 325-340.
- Stive, M.J.F. and H.J. DeVriend, 1987. Onasi 3-D nearshore current modelling: wave-induced secondary currents, in *Proc. of Special Conference on Coastal Hydrodynamics*, ASCE, New York, 356-370.
- Svendsen, I.A., 1984. Mass flux and undertow in a surf zone. *Coastal Engineering*, *8*, 347-365.
- Svendsen, I.A. and R.S. Lorenz, 1988. Three dimensional flow profiles on littoral beaches. *Proc. Twenty-first Coastal Engineering Conference*, ASCE, New York, 705-717.
- Thornton, E.B. and R.T. Guza, 1983. Transformation of wave height distribution. *J. Geophys. Res.*, *88*, 5925-5938.